

Early changes in the extracellular matrix of the degenerating intervertebral disc, assessed by Fourier transform infrared imaging.

EMANUEL, Kaj S, MADER, Kerstin T <<http://orcid.org/0000-0002-2524-6512>>, PEETERS, Mirte, KINGMA, Idsart, RUSTENBURG, Christine M E, VERGROESEN, Pieter-Paul A, SAMMON, Christopher <<http://orcid.org/0000-0003-1714-1726>> and SMIT, Theodoor H

Available from Sheffield Hallam University Research Archive (SHURA) at:
<https://shura.shu.ac.uk/21746/>

This document is the Accepted Version [AM]

Citation:

EMANUEL, Kaj S, MADER, Kerstin T, PEETERS, Mirte, KINGMA, Idsart, RUSTENBURG, Christine M E, VERGROESEN, Pieter-Paul A, SAMMON, Christopher and SMIT, Theodoor H (2018). Early changes in the extracellular matrix of the degenerating intervertebral disc, assessed by Fourier transform infrared imaging. Osteoarthritis and cartilage. [Article]

Copyright and re-use policy

See <http://shura.shu.ac.uk/information.html>

Early changes in the extracellular matrix of the degenerating intervertebral disc, assessed by Fourier transform infrared imaging

Kaj S. Emanuel^{a,b}, Kerstin T. Mader^c, Mirte Peeters^b, Idsart Kingma^d, Christine M.E.
Rustenburt^{a,b}, Pieter-Paul A. Vergroesen^{b,e}, Christopher Sammon^c, Theodoor H. Smit^{a,f,*}

*corresponding author

a - Department of Orthopaedic Surgery, Academic Medical Center, University of Amsterdam,
Amsterdam Movement Sciences, Amsterdam, The Netherlands.

b – Department of Orthopedic Surgery, VU University Medical Center, Amsterdam
Movement Sciences, The Netherlands

c – Materials and Engineering Research Institute, Sheffield Hallam University, Sheffield, UK

d – Department of Human Movement Sciences, Vrije Universiteit Amsterdam, Amsterdam
Movement Sciences, The Netherlands

e – Department of Orthopaedic Surgery, NoordWest Ziekenhuisgroep, Alkmaar, The
Netherlands

f – Department of Medical Biology, Academic Medical Center, University of Amsterdam,
Amsterdam Movement Sciences, Amsterdam, The Netherlands.

*Corresponding author at: Academisch Medisch Centrum, Postbus 22660, 1100DD
Amsterdam, The Netherlands, tav. prof. dr. ir. T.H. Smit, Department of Medical Biology,
t.h.smit@amc.uva.nl

Other authors:

Kaj Emanuel: k.s.emanuel@amc.uva.nl

Kirsten Mader: k.mader@shu.ac.uk

Mirte Peeters: m.peeters@vumc.nl

Idsart Kingma: i.kingma@vu.nl

Christine Rustenburg: c.rustenburg@vumc.nl

Pieter-Paul Vergroesen: pvergroesen@gmail.com

Christopher Sammon: c.sammon@shu.ac.uk

Running Title: Early matrix changes with disc degeneration

Abstract

Objective: Mechanical overloading induces a degenerative cell response in the intervertebral disc. However, early changes in the extracellular matrix (ECM) are challenging to assess with conventional techniques. Fourier Transform Infrared (FTIR) imaging allows visualization and quantification of the ECM. We aim to identify markers for disc degeneration and apply these to investigate early degenerative changes due to overloading and catabolic cell activity.

Design: Three experiments were conducted; Exp 1.: *In vivo*, lumbar spines of seven goats were operated: one disc was injected with chondroitinase ABC (mild degeneration) and compared to the adjacent disc (control) after 24 weeks. Exp 2a.: *Ex vivo*, caprine discs received physiological loading (n=10) or overloading (n=10) in a bioreactor. Exp 2b.: Cell activity was diminished prior to testing by freeze-thaw cycles, 18 discs were then tested as in Exp 2a. In all experiments, FTIR images (spectral region: 1000-1300 cm^{-1}) of mid-sagittal slices were analyzed using multivariate curve resolution.

Results: *In vivo*, FTIR was more sensitive than biochemical and histological analysis in identifying reduced proteoglycan content ($p=0.046$) and increased collagen content in degenerated discs ($p<0.01$). Notably, FTIR analysis additionally showed disorganization of the ECM, indicated by increased collagen entropy ($p=0.011$).

Ex vivo, the proteoglycan/collagen ratio decreased due to overloading ($p=0.047$) and collagen entropy increased ($p=0.047$). Cell activity affected collagen content only ($p=0.044$).

Conclusion: FTIR imaging allows a more detailed investigation of early disc degeneration than traditional measures. Changes due to mild overloading could be assessed and quantified.

Matrix remodeling is the first detectable step towards intervertebral disc degeneration.

Keywords: Fourier transform infrared; spectroscopy; intervertebral disc degeneration; overloading; collagen; entropy

Introduction

Intervertebral disc degeneration is a major cause of low-back pain¹, which causes the most years lived with disability worldwide². It is accepted that accumulating biomechanical overloading can initiate intervertebral disc degeneration^{3,4}, but the pathophysiology is still under debate. On the one hand, it has been suggested that “repetitive loading can create microscopic damage within a material or tissue which gradually builds up until gross failure occurs”⁵. This assumes a passive role of the chondrocyte-like cells, which repair minor tissue damage, but would be unable to keep up with gross failure⁶. On the other hand, based on the many other factors that contribute to intervertebral disc degeneration (e.g. nutrient shortage, systemic inflammation, smoking), we hypothesized that disc degeneration is a vicious cycle⁷, where living cells interact with mechanical loading and extracellular matrix in a positive feedback loop (see Fig. 1). This is suggested by the observation that mild overloading of healthy intervertebral discs in a bioreactor results in catabolic (MMP13, ADAMTS5) and inflammatory gene expressions (IL-1, IL-8) by the resident chondrocytes⁸. Early changes in the extracellular matrix, however, are subtle and difficult to quantify by histology or magnetic resonance imaging (MRI).

Fourier transform infrared (FTIR) imaging was recently introduced as a method to visualize extracellular matrix composition of intervertebral discs on a tissue section without the need for staining⁹. With this method, the absorption of a range of frequencies of infrared light by thin slices of tissue is mapped. As different chemical bonds absorb light at different frequencies, information regarding the chemical composition can be obtained. This has several advantages over traditional histology, as this allows objective and quantitative measurement of the extracellular matrix composition. When the raw data can be deconvoluted into the dominant extracellular matrix types, such as proteoglycans and collagens, the distribution can be assessed in 2D on the same tissue sections, allowing ratio calculations. This has several advantages over the analysis of digitized histological staining. First, chemical contrast is generated without staining, which is therefore less affected by multiple sources of variations due to e.g. staining preparation and handling differences¹⁰. Furthermore, multiple ECM types can be quantified on the same slice, which enables ratio calculation. Altogether, FTIR imaging is a promising method to study more subtle changes in extracellular matrix than traditional measures, which would be necessary to study early changes with degeneration.

In this study, we first aimed to identify markers for degeneration based on FTIR imaging, using a validated *in vivo* goat model of mild degeneration^{11,12}. The use of this model was necessary because healthy human control discs are rarely available for research. Secondly, we aimed to use these markers to detect early degenerative changes in *ex vivo* overloaded healthy goat intervertebral discs. We previously found upregulation of remodeling genes and downregulation of proteoglycan genes⁸. Here we hypothesize that proteoglycan content and structural integrity of the extracellular matrix are reduced in both the *in vivo* mildly degenerated discs and in the *ex vivo* overloaded discs. Our third aim was to assess the role of cell activity in early degeneration due to overloading. To that end, the *ex vivo* overloading experiment was repeated in an additional group while the cell activity was repressed in advance by freeze-thaw cycles. Since we hypothesize that changes in the extracellular matrix in response to overloading are cell-mediated (see Fig. 1), we expect less degenerative changes due to overloading in the group with suppressed cell activity.

Methods

Experiment 1: in vivo degeneration with cABC

Approval of the research protocol was obtained from the Animal Ethics Committee of the VU University Medical Center. Reporting of the experiment was conducted according to ARRIVE guidelines¹³. In each of seven healthy adult Dutch milk goats (age: 3.8 ± 1.5 years), one lumbar intervertebral disc was injected with 0.25U chondroitinase ABC (cABC) per mL PBS in the nucleus pulposus using a 29G needle in the nucleus pulposus. This is a validated model for mild intervertebral disc degeneration^{11,12}, as cABC cleaves proteoglycans in the nucleus pulposus. In every spine examined, one lumbar intervertebral disc served as a healthy control and was untreated. This resulted in seven healthy control discs and seven degenerated discs, which were used in this study. The goats were originally part of a treatment study, in which four additional lumbar discs received cABC injection and a hydrogel treatment twelve weeks later. After 12 more weeks, the goats were sacrificed. This study has been reported elsewhere¹⁴.

Midsagittal slices of the intervertebral discs were fixed in 4% formalin for 10 days, decalcified in Kristensens fluid for a week, embedded in paraffin, cut into 2 μ m sections and mounted onto stainless steel slides. Nucleus pulposus and annulus fibrosis material of the

remaining tissue was obtained for quantitative biochemistry. Glycosaminoglycan (GAG) content was measured using a 1.9-dimethyl-methylene blue (DMMB) assay (Biocolor Ltd) according to manufacturers' instructions. Hydroxyproline (HYP) content, a measure for total collagen content, was determined using a dimethylamino-benzaldehyde (DMBA) hydroxyproline assay. Histological analysis was done via Alcian Blue and H&E staining of midsagittal slices on a 6-point scale using the methods described elsewhere¹⁵.

FTIR

Mid-infrared spectroscopic images of the section on steel slides were measured with an Agilent 680-IR FTIR spectrometer, coupled to an Agilent 620-IR FTIR imaging microscope. The microscope was coupled with a liquid nitrogen cooled 64×64 mercury–cadmium–telluride focal plane array detector (FPA). Transflectance FTIR mosaic images (23×57 images, pixel aggregation 256, image pixel dimensions: 92×228) were collected with a 4 cm^{-1} spectral resolution.

After manual exclusion of the bony parts, all scans were collated to one large data matrix. Data was pre-processed with custom-built code in MATLAB R2017a (IBM, The Mathworks, Inc., Natick, MA, USA). In summary, a second derivative was performed on the spectra (Savitzky–Golay: order 3, length 15). Furthermore, a tissue map was generated based on integration of the Amide III region ($1297\text{--}1186 \text{ cm}^{-1}$) in order to correct for tissue thickness variations. The data matrices were analyzed using a multivariate statistical methodology described by Mader *et al.*⁹ They applied a MCR-ALS algorithm, which uses non-linear iterative partial least squares (NIPALS) decomposition and iterative alternating least-square optimization with soft non-negative constraints¹⁶ (MCRv1.6 Copyright© 2003–2004 Unilever, UK). MCR-ALS analysis was carried out in a wavenumber range of $1000\text{--}1300 \text{ cm}^{-1}$ using the following settings: number of factors: 2; maximum number of iterations: 500; constraints: MALS-2D. The analyzed wavenumber region includes proteoglycan (SO_3^- antisymmetric stretching vibration, C-O stretching vibrations, C-O-S antisymmetric stretching vibrations) and collagen (amide III vibrations, C-O stretching vibrations) specific bonds,¹⁷ which were used to determine the chemical identity of MCR-ALS factors. Additionally, calculated spectral MCR-ALS profiles were compared to the spectral profiles of reference materials collagen I, collagen II, chondroitin sulfate A, sodium salt and hyaluronic acid (all bovine) obtained from Sigma Aldrich (Gillingham, Dorset, UK). More details on the data analysis have been described elsewhere⁹. The calculated factors were averaged over the caudal-cranial

axis for 1D visualization and quantitative comparison. Further averaging over the anterior-posterior axis was used to obtain the average content of a matrix type. The structures were separated in nucleus pulposus and annulus fibrosis by manual selection of the region of interest (ROI) on the tissue map based on visual inspection. To quantify the disorganization of the collagen matrix, the distribution of the entire slice was analyzed by calculating the entropy, a standard texture analysis method of MATLAB. The entropy is defined as in Equation 1:

$$Entropy = -\sum(p * \log_2(p)) \quad \text{Equation 1}$$

Where p contains the normalized histogram counts of the intensity of the MCR image factor. To analyze the local variations of the entropy, each intervertebral disc was divided in 10 equal parts from anterior to posterior, and the entropy was calculated for each part separately.

Experiment 2a: ex vivo degeneration using overloading

Five spines of healthy Dutch Milk Goats were obtained from a local slaughterhouse. Within a few hours post-mortem, five lumbar intervertebral discs were removed from each spine (n=25) using an oscillating saw. Sawing debris was removed by flushing with PBS. One disc from each spine (n=5) did not receive any treatment and was immediately fixed in formaldehyde (t=0) after removal from the spine. The other four discs (n=20) were implemented in culture chambers of a custom-build Loaded Disc Culture System (LDCS). This LDCS allows application of axial compressive load to the intervertebral discs, as well as a constant flow of culture medium¹⁸. The intervertebral discs were cultured in standard culture medium (DMEM, Life Technologies) with added 10% Hyclone fetal bovine serum (FBS, Thermo Scientific), 1% PSF, 3.5 g/L glucose (Merck), 25 mM HEPES buffer (Life Technologies) and 50 µg/ml ascorbate-2-phosphate (Sigma Aldrich).

From each spine, two randomly selected intervertebral discs were subjected to physiological loading (n=10), and two to overloading (n=10). Physiological loading was defined previously based on cage measures *in vivo* and was validated as a loading regime that maintained cell vitality, and induced no changes in gene expressions over the course of three weeks¹⁸. The physiological loading consisted of a dynamic daily regime of 8 hours of night time Low Dynamic Load (LDL) of 50 ± 10 N, and then 16 hours of alternating 30 minutes of LDL and High Dynamic Load (HDL) of 150 ± 100 N. The overloading loading regime is the same as

the physiological loading, except that the HDL phases are doubled in average force to 300 ± 100 N. The overloading was previously shown to induce katabolic and inflammatory gene expression⁸.

After three weeks of culturing with loading, the intervertebral discs were removed and midsagittal slices were mounted onto steel slides as in experiment 1. FTIR images were obtained as in experiment 1, other than that the microscope was coupled with a new larger 128 x 128 FPA detector. Slices from the same intervertebral discs were processed for histological analysis using H&E, Safranin O and Masson's Trichrome staining. The sections were graded for degeneration by two independent observers, both using two different histological scales for intervertebral disc degeneration^{15,19}.

Experiment 2b: reduced cell viability

Experiment 2a was replicated with reduced cell viability, to test whether effects observed were due to cell activity. This is because extracellular matrix changes can occur in two ways: direct tissue damage due to the mechanical wear-and-tear, and biological adaptation due to mechanobiological cell activity. In order to address this, five additional lumbar goat spines were frozen at -20 °C for at least a month, including three freeze-thaw cycles. This group will be referred to as "non-vital", as cell viability is known to decrease drastically with this treatment²⁰. The non-vital group was cultured in Phosphate Buffered Saline (PBS, Sigma Aldrich) only, with similar osmotic properties to culture medium, with 1% PSF added to prevent infection. All other steps and loading regimes were the same as applied to the vital group (Experiment 2a). If the changes with overloading, seen in Experiment 2a, do not occur in the group with reduced cell activity, the changes can be attributed to cell activity. If they do occur, it is due to mechanical wear-and-tear.

Statistics

All statistical tests were performed in SPSS Statistics for Windows (Version 22; IBM Corp., Armonk, NY). For each experiment, normality of the distribution of the FTIR parameters (average intensity or entropy) was investigated by visual inspection of QQ-plots and Shapiro-Wilk tests. The difference between parameters in experiment 1 was evaluated using a paired t-test, comparing the control and degenerated disc within each goat. The difference in histological score was evaluated using a signed rank test. The influence of loading regime on FTIR parameters in experiment 2a was analyzed using a linear mixed model. The model

included loading regime as fixed factor, because this is the independent variable we are interested in. It also included a random effect for each goat as a grouping factor, because multiple discs of each goat received the same loading regime, and therefore the discs within one subject are not independent. For experiment 2b, with the non-vital group added, vitality was added as fixed factor, as well as the interaction between loading group and vitality. This interaction models the influence of cell vitality on the effect of overloading. The difference between groups in the histological scores was evaluated using a Kruskal-Wallis test by ranks.

Results

Experiment 1

The increase in degeneration in the cABC injected discs compared to the control was confirmed on a 6-point histological grading score (median score [range]: 1 [0-4] vs 3 [1-5], $p=0.031$). Based on the GAG-assay of nucleus pulposus material, however, the difference between degenerated and control was not significant (365 vs 290 ug/mg $p=0.11$). The differences between groups in the HYP content (25.6 vs 29.1 ug/mg, $p=0.54$) and the GAG/HYP ratio (18.1 vs 11.1 g/g, $p=0.21$) were not statistically significant. These data were reported elsewhere previously¹⁴.

In the FTIR MCR-ALS component analysis two factors for specific ECM types were identified. One factor showed the distribution of proteoglycans over the intervertebral disc. The average proteoglycan content in the nucleus showed a strong correlation ($r=0.74$, $p<0.01$) with GAG content, measured with the bio-assay. The second factor that could be identified had a clear spectroscopic match with FTIR profiles of reference materials collagen-I and collagen-II (Fig. 2). The correlation between average collagen factor and hydroxyproline content was moderate ($r=0.54$, $p<0.05$). An overlay plot of the distribution of collagen and proteoglycan across the discs is shown in Fig. 3.

The average extracellular matrix content over the anterior-posterior axis is shown in Fig. 4. As expected, relatively more proteoglycan is found in the nucleus area, while more collagen is present in the outer annulus areas. All hereafter mentioned FTIR parameters (average intensity or entropy) were normally distributed. In the degenerated intervertebral discs, significantly less average proteoglycan was found compared to control discs, both overall ($p=0.046$) and in the nucleus area ($p=0.047$). The average collagen content was higher

($p<0.01$) in the degenerated discs, both in the nucleus ($p=0.027$) and anterior annulus ($p<0.01$) (See Table 1). As a result, the proteoglycan/collagen ratio was also significantly reduced in degenerated discs compared to control, both overall ($p=0.017$) and in the anterior annulus ($p=0.018$). To test for disorganization of the collagen matrix, the distribution was analyzed by calculating the entropy. The collagen entropy was significantly higher in the degenerated discs ($p=0.011$). This means that a decrease of collagen organization is found in the degeneration group. The difference between the groups was most pronounced in the nucleus pulposus and anterior annulus areas (Table 3). A similar test of proteoglycan entropy differences did not reveal significant differences between the control and degenerated groups ($p=0.70$). Based on these results, the following FTIR markers for degeneration were selected for experiment 2: average proteoglycan content, increased collagen content, reduced proteoglycan/collagen ratio and increased collagen entropy.

Experiment 2a

Due to damage to intervertebral discs during dissection and tissue damage during preparation for histology, analysis could not be completed for 2 intervertebral discs; therefore 23 intervertebral discs remained.

No statistically significant differences between control loading, overloading, and $t=0$ (directly after sacrifice) were found in the scores based on conventional histological staining with Safranin O and H&E (Table 2, Fig. 5). All assessed FTIR parameters showed a normal distribution. The overloaded intervertebral discs had significantly higher collagen entropy than the control loaded intervertebral discs ($p=0.047$). No significant difference in overall average proteoglycan content ($p=0.20$), or collagen content ($p=0.15$) was found between the overloaded and control loaded discs (Fig. 6). However, the proteoglycan/collagen ratio was significantly lower in the overloaded group ($p=0.047$). Only whole-disc differences were significant. No significant difference between the control loaded group and the $t=0$ group was found in collagen or proteoglycan content or entropy (all $p>0.05$), although there was a trend towards higher collagen content in the control loaded group ($p=0.075$).

Experiment 2b

To test whether cell activity modulates the effect of overloading, the experiment was replicated with the same loading conditions, but with reduced cell viability. In total, 18 intervertebral discs were added to the analysis, in addition to the discs of experiment 2a. In

this extended dataset, significant main effects of overloading compared to control loading were found for collagen entropy ($p=0.038$), average collagen content ($p=0.036$) and average proteoglycan/collagen ratio ($p=0.006$). The interaction between loading and vitality was only significant for the average collagen content ($p=0.044$), with a trend towards an interaction for average proteoglycan/collagen ratio ($p=0.059$), but not for proteoglycan content ($p=0.67$) or collagen entropy ($p=0.30$).

Discussion

Previously, it was shown that it was possible to detect several extracellular matrix types using FTIR imaging⁹. In the current study, the analysis of intervertebral discs was further developed to allow analysis of early disc degeneration, for which insufficiently sensitive markers exist to date. It was found that, from FTIR spectroscopic images of mid-sagittal slices, mild disc degeneration is related to reduced proteoglycan content, increased collagen content, and increased collagen entropy. Furthermore, after only three weeks of mild biomechanical overloading, a significant increase in entropy of the collagen factor and a decrease of average proteoglycan/collagen ratio could be detected. This indicates that the first steps into the vicious cycle of degeneration are related to the remodeling of the matrix, with a shift from proteoglycan-rich tissue to more fibrous collagen-rich tissue. At the same time, the organization in the collagen matrix is decreasing, as shown by an increase in entropy. The hypothesis that these changes are cell-mediated was not convincingly confirmed, as only the average collagen factor showed a significant interaction between the loading and vitality group; this implies that we found only minor support for a different response to loading due to reduced cell activity.

Control discs were compared to intervertebral discs treated with cABC injection to induce mild degeneration, a model that has been validated in several studies^{11,12,21}. FTIR imaging showed a greater sensitivity to find differences between groups compared to traditional measures like histological grading and bio-assays. Possibly, the tissue samples for the bio-assay, taken from pieces of nucleus pulposus and annulus fibrosis just outside the midsagittal plane, were less representative compared to complete midsagittal slices. Furthermore, the GAG-assay only binds to the sulfated chains of proteoglycans, while the FTIR spectral signature includes the backbone and other non-sulfated proteoglycans, such as hyaluronic acid.

The proteoglycan-to-collagen ratio has been widely used as a marker for degenerative changes^{11,22,23}. Using FTIR imaging, we found that with *in vivo* degeneration the proteoglycan factor/collagen factor ratio in the nucleus pulposus was reduced from 8.1 (control) to 3.7 (mild degeneration). A statistically insignificant reduction was measured with the GAG/HYP assays: 18 vs 11. However, GAG/HYP ratio is an indirect measure for proteoglycan to collagen ratio, as GAG and HYP are only a small part of the proteoglycan and collagen molecules.

The most significant drawback of the current protocol is that the tissue is fixed in formaldehyde, which has a big absorption peak at 1460 cm^{-1} , making it very difficult to include this region in the analysis, as the peak dominates the component analysis. However, the differences between the collagen type-I and type-II reference measurements are located exactly in this region⁹. A different conservation technique may improve the possibilities of matrix component identification. We speculate that the increase in collagen factor with degeneration, as found in this study, could be attributed to type-I collagen, as in previous work a strong upregulation of gene expression of collagen type-I in the nucleus pulposus was found with overloading, while the expression for collagen type-II was reduced⁸. The increase in entropy of the collagen factor may be a combination of newly formed collagen that is less attached to the highly-organized annulus fibrosis, and to the damaged collagen due to mechanical wear-and-tear or enzymatic cleavage. Future experiments with polarized light to determine the local orientation of the fibers, combined with immunohistochemical staining of multiple collagen types, may determine the contributions of the different processes. Recently, two studies were published that investigated the relation between degeneration and the heterogeneity of MRI signals in the intervertebral disc^{24,25}, both indicating that the disorder of the extracellular matrix of the intervertebral disc is a relevant measure for disc degeneration. Furthermore, the intensity of the T2 signal on MRI, commonly used to determine disc degeneration, is dependent on the integrity and orientation of collagen fibers^{26,27}. Therefore, the reduction in T2 signal, as found with mild degeneration²⁸ could be partly attributed to the increasing entropy of the collagen network.

The effect of overloading on the matrix of the intervertebral disc was subtle in this study, as traditional histology could not distinguish between overloaded and control-loaded groups. This was unexpected, as previous work did show a significant difference in gene expressions that indicated remodeling of the matrix⁸. Matrix breakdown is however a slow process,

because the cell density in the intervertebral disc is very low²⁹. The turnover rate for proteoglycans in the intervertebral disc is estimated at roughly 5% per year³⁰; for collagen, rates between 0.3 and 0.7 % are reported³¹. Therefore, an overloading period longer than three weeks or a more intense overloading regime may be needed for future studies to provide a more robust outcome.

The hypothesis that initiation of intervertebral disc degeneration is cell-mediated was not confirmed. If the effect of overloading is different in the vital groups compared to the non-vital groups, this would be expressed in the statistical model as an interaction between loading group and vitality. In the measures which were significantly different between the overloading and control loading in the vital intervertebral discs, no significant interaction was found. The average collagen factor content did show a significant interaction, which is not surprising when considering that cell activity is needed to increase the collagen content. It is unclear, however, if the increase in collagen entropy and break-down of proteoglycans, as observed in the vital group, are also mediated by cell activity. The absence of the interaction between loading group and vitality in these measures did not indicate that. The vitality was reduced by three freeze-thaw cycles, and the cell activity was further reduced by culturing on PBS instead of culture medium. Three freeze-thaw cycles at -20 °C was shown to kill 100% of chondrocytes in articular cartilage²⁰.

The transferability of the spectral factors between the *in vivo* experiment and the bioreactor studies, despite a slightly different scanning setup, is an important finding, as this is a requirement for wider implementation. A limitation in the current study is the use of goat intervertebral discs. The use of an animal model is necessary in the study of healthy intervertebral discs, as healthy human tissue is not readily available. The bioreactor studies reduce the use of animal models, as only waste products of the slaughterhouse are needed. The goat is used as a model because goat intervertebral discs do not contain notochordal cells, similar to the adult human intervertebral disc³². Furthermore, quadrupeds are a useful model biomechanically, despite their horizontal alignment³³. For the application of the load on the intervertebral discs in the bioreactor, it was decided to not correct for size of the disc, as the mid-sagittal area was unknown at before the start of the experiments and the bone area may not be a reliable estimate of size differences. In previous research with the same goat population, the mid-sagittal area differences were relatively small: $4.35 \pm 0.46 \text{ cm}^2$.³⁴ Furthermore, no bias was introduced as intervertebral discs were randomly allocated to the

different groups. Another limitation is that the FTIR measures in this study have no unit, and are therefore not directly comparable to other studies. Future studies on the relation between these measures and proteoglycan and collagen concentration should enable the conversion to actual concentration. Another important limitation is that this method is not applicable in the clinical setup, as intervertebral disc tissue cannot be obtained without damaging the intervertebral disc. There is a great need for the improvement of current clinical imaging of intervertebral disc degeneration. The currently most-used clinical imaging method, the MRI-based Pfirrmann Score³⁵, is widely regarded as unsatisfactory due to low discriminative power and subjective nature^{36,37}. However, to improve this gold standard, new MRI techniques need to be validated against relevant, quantitative measures for intervertebral disc degeneration, which are currently unavailable. Developing measures that can be used in research will eventually facilitate the improvement of clinical measures. With FTIR spectroscopic imaging it is possible to describe the process of degeneration in a more detailed and quantitative manner, and therefore it could serve as a potential benchmark for clinical imaging methods.

In conclusion, FTIR imaging provides quantitative, sensitive measures to study early changes in extracellular matrix with intervertebral disc degeneration. This is an important step forward, as such measures are necessary to be able to study the etiology of intervertebral disc or cartilage degeneration. Reduction in proteoglycan factor, increase in collagen factor, decrease of the proteoglycan/collagen ratio and increase in the collagen entropy were shown to be measures for intervertebral disc degeneration. After three weeks of overloading, the proteoglycan/collagen factor ratio was reduced, and the collagen entropy increased. Our study is inconclusive about whether this process is cell-mediated.

Role of funding sources.

The authors acknowledge the financial support of the Task Force of Research of EUROSPINE and COST-Action MP1302: Nanospectroscopy. The sponsors were not involved in the experiment or manuscript submission.

Competing interests

None of the authors reported conflicts of interest.

Author contributions

KE, PV, IK, MP & TS designed the experiments. KE, MP & CR conducted the experiments. KE, KM & CS performed FTIR analysis. KE, IK, KM, CS & TS analyzed overall results. KE drafted the manuscript. All authors critically reviewed the manuscript and approved the final version.

References

1. Brinjikji W, Diehn F, Jarvik J, Carr C, Kallmes DF, Murad MH, et al. MRI findings of disc degeneration are more prevalent in adults with low back pain than in asymptomatic controls: a systematic review and meta-analysis. *American Journal of Neuroradiology*. 2015;36(12):2394-2399. 10.3174/ajnr.A4498
2. Vos T, Flaxman AD, Naghavi M, Lozano R, Michaud C, Ezzati M, et al. Years lived with disability (YLDs) for 1160 sequelae of 289 diseases and injuries 1990–2010: a systematic analysis for the Global Burden of Disease Study 2010. *The Lancet*. 2013;380(9859):2163-2196.
3. Chan SC, Ferguson SJ, Gantenbein-Ritter B. The effects of dynamic loading on the intervertebral disc. *Eur Spine J*. 2011;20(11):1796-1812. 10.1007/s00586-011-1827-1
4. Hung YJ, Shih TT, Chen BB, Hwang YH, Ma LP, Huang WC, et al. The dose-response relationship between cumulative lifting load and lumbar disk degeneration based on magnetic resonance imaging findings. *Phys Ther*. 2014;94(11):1582-1593. 10.2522/ptj.20130095
5. Adams MA. Biomechanics of back pain. *Acupuncture in Medicine*. 2004;22(4):178-188. 10.1136/aim.22.4.178
6. Coenen P, Kingma I, Boot CR, Bongers PM, van Dieën JH. The contribution of load magnitude and number of load cycles to cumulative low-back load estimations: a study based on in-vitro compression data. *Clinical Biomechanics*. 2012;27(10):1083-1086. 10.1016/j.clinbiomech.2012.07.010
7. Vergroesen PP, Kingma I, Emanuel KS, Hoogendoorn RJ, Welting TJ, van Royen BJ, et al. Mechanics and biology in intervertebral disc degeneration: a vicious circle. *Osteoarthritis Cartilage*. 2015;23(7):1057-1070. 10.1016/j.joca.2015.03.028
8. Paul CP, Schoorl T, Zuiderbaan HA, Zandieh Doulabi B, van der Veen AJ, van de Ven PM, et al. Dynamic and static overloading induce early degenerative processes in caprine lumbar intervertebral discs. *PLoS One*. 2013;8(4):e62411. 10.1371/journal.pone.0062411
9. Mader KT, Peeters M, Detiger SE, Helder MN, Smit TH, Le Maitre CL, et al. Investigation of intervertebral disc degeneration using multivariate FTIR spectroscopic imaging. *Faraday discussions*. 2016;187:393-414. 10.1039/c5fd00160a
10. Hyllested J, Veje K, Ostergaard K. Histochemical studies of the extracellular matrix of human articular cartilage—a review. *Osteoarthritis and cartilage*. 2002;10(5):333-343.
11. Hoogendoorn RJ, Helder MN, Kroeze RJ, Bank RA, Smit TH, Wuisman PI. Reproducible long-term disc degeneration in a large animal model. *Spine*. 2008;33(9):949-954. 10.1097/BRS.0b013e31816c90f0
12. Gullbrand S, Malhotra N, Schaer T, Zawacki Z, Martin J, Bendigo J, et al. A large

- animal model that recapitulates the spectrum of human intervertebral disc degeneration. *Osteoarthritis and Cartilage*. 2017;25(1):146-156. 10.1016/j.joca.2016.08.006
13. Kilkenny C, Browne WJ, Cuthill IC, Emerson M, Altman DG. Improving bioscience research reporting: the ARRIVE guidelines for reporting animal research. *PLoS biology*. 2010;8(6):e1000412.
14. Peeters M, Detiger SE, Karfeld-Sulzer LS, Smit TH, Yayon A, Weber FE, et al. BMP-2 and BMP-2/7 heterodimers conjugated to a fibrin/hyaluronic acid hydrogel in a large animal model of mild intervertebral disc degeneration. *BioResearch open access*. 2015;4(1):398-406. 10.1089/biores.2015.0025
15. Hoogendoorn RJ, Wuisman PI, Smit TH, Everts VE, Helder MN. Experimental intervertebral disc degeneration induced by chondroitinase ABC in the goat. *Spine*. 2007;32(17):1816-1825. 10.1097/BRS.0b013e31811ebac5
16. Wang J-H, Hopke PK, Hancewicz TM, Zhang SL. Application of modified alternating least squares regression to spectroscopic image analysis. *Analytica Chimica Acta*. 2003;476(1):93-109.
17. Rieppo L, Saarakkala S, Narhi T, Helminen HJ, Jurvelin JS, Rieppo J. Application of second derivative spectroscopy for increasing molecular specificity of Fourier transform infrared spectroscopic imaging of articular cartilage. *Osteoarthritis Cartilage*. 2012;20(5):451-459. 10.1016/j.joca.2012.01.010
18. Paul CP, Zuiderbaan HA, Zandieh Doulabi B, van der Veen AJ, van de Ven PM, Smit TH, et al. Simulated-physiological loading conditions preserve biological and mechanical properties of caprine lumbar intervertebral discs in ex vivo culture. *PLoS One*. 2012;7(3):e33147. 10.1371/journal.pone.0033147
19. Sive J, Baird P, Jeziorski M, Watkins A, Hoyland J, Freemont A. Expression of chondrocyte markers by cells of normal and degenerate intervertebral discs. *Molecular Pathology*. 2002;55(2):91.
20. Clements K, Bee Z, Crossingham G, Adams M, Sharif M. How severe must repetitive loading be to kill chondrocytes in articular cartilage? *Osteoarthritis and Cartilage*. 2001;9(5):499-507. 10.1053/joca.2000.0417
21. Detiger SE, Hoogendoorn RJ, van der Veen AJ, van Royen BJ, Helder MN, Koenderink GH, et al. Biomechanical and rheological characterization of mild intervertebral disc degeneration in a large animal model. *J Orthop Res*. 2013;31(5):703-709. 10.1002/jor.22296
22. Emanuel KS, Vergroesen P-PA, Peeters M, Holewijn RM, Kingma I, Smit TH. Poroelastic behaviour of the degenerating human intervertebral disc: a ten-day study in a loaded disc culture system. *European Cells and Materials*. 2015;29:330-341. 10.22203/eCM.v029a25
23. Mwale F, Roughley P, Antoniou J. Distinction between the extracellular matrix of the nucleus pulposus and hyaline cartilage: a requisite for tissue engineering of intervertebral disc. *Eur Cell Mater*. 2004;8(58):63-64. 10.22203/eCM.v008a06
24. Waldenberg C, Hebelka H, Brisby H, Lagerstrand KM. MRI histogram analysis enables objective and continuous classification of intervertebral disc degeneration. *European Spine Journal*. 2017:Pub. ahead of Print. 10.1007/s00586-017-5264-7
25. Pandit P, Talbott JF, Pedoia V, Dillon W, Majumdar S. T1ρ and T2-based characterization of regional variations in intervertebral discs to detect early degenerative changes. *Journal of Orthopaedic Research*. 2016;34(8):1373-1381.
26. Xia Y, Farquhar T, Burton-Wurster N, Lust G. Origin of cartilage laminae in MRI. *Journal of Magnetic Resonance Imaging*. 1997;7(5):887-894.
27. Shao H, Pauli C, Li S, Ma Y, Tadros AS, Kavanaugh A, et al. Magic angle effect

- plays a major role in both T1rho and T2 relaxation in articular cartilage. *Osteoarthritis and Cartilage*. 2017;25(12):2022-2030. 10.1016/j.joca.2017.01.013
28. Luoma K, Vehmas T, Riihimäki H, Raininko R. Disc height and signal intensity of the nucleus pulposus on magnetic resonance imaging as indicators of lumbar disc degeneration. *Spine*. 2001;26(6):680-686. Doi 10.1097/00007632-200103150-00026
29. Liebscher T, Haefeli M, Wuertz K, Nerlich AG, Boos N. Age-related variation in cell density of human lumbar intervertebral disc. *Spine*. 2011;36(2):153-159.
30. Sivan SS, Tsitron E, Wachtel E, Roughley PJ, Sakke N, van der Ham F, et al. Aggrecan turnover in human intervertebral disc as determined by the racemization of aspartic acid. *Journal of Biological Chemistry*. 2006;281(19):13009-13014.
31. Sivan S-S, Wachtel E, Tsitron E, Sakke N, van der Ham F, DeGroot J, et al. Collagen turnover in normal and degenerate human intervertebral discs as determined by the racemization of aspartic acid. *Journal of Biological Chemistry*. 2008;283(14):8796-8801.
32. Vonk LA, Kroeze RJ, Doulabi BZ, Hoogendoorn RJ, Huang C, Helder MN, et al. Caprine articular, meniscus and intervertebral disc cartilage: an integral analysis of collagen network and chondrocytes. *Matrix Biol*. 2010;29(3):209-218. 10.1016/j.matbio.2009.12.001
33. Smit TH. The use of a quadruped as an in vivo model for the study of the spine - biomechanical considerations. *Eur Spine J*. 2002;11(2):137-144. 10.1007/s005860100346
34. Emanuel KS, van der Veen AJ, Rustenburg CM, Smit TH, Kingma I. Osmosis and viscoelasticity both contribute to time-dependent behaviour of the intervertebral disc under compressive load: A caprine in vitro study. *Journal of Biomechanics*. 2017;70:10-15.
35. Pfirrmann CW, Metzdorf A, Zanetti M, Hodler J, Boos N. Magnetic resonance classification of lumbar intervertebral disc degeneration. *Spine*. 2001;26(17):1873-1878.
36. Adams MA, Roughley PJ. What is intervertebral disc degeneration, and what causes it? *Spine*. 2006;31(18):2151-2161.
37. Videman T, Battié MC, Gibbons LE, Gill K. A new quantitative measure of disc degeneration. *The Spine Journal*. 2017;17(5):746-753. 10.1016/j.spinee.2017.02.002

Figure 1. The vicious cycle of intervertebral disc degeneration. Biomechanical signals can induce cellular remodeling of the extracellular matrix, which in turn changes the biomechanical properties. Reprinted from Vergroesen et al.,⁷ with permission from Elsevier.

Figure 2. Left: Spectral profiles of proteoglycan factor, received from the MCR analysis of experiment 1, compared to spectral profiles of reference hyaluronic acid and chondroitin sulfate. Right: spectral profile of collagen with reference measurements of pure collagen I and II.

Figure 3. Example of overlay plots of proteoglycan factor (green) and collagen factor (red), scaled on RGB from 0 to 255 (255 is the highest value seen in all intervertebral discs).

Figure 4. Average distribution of the proteoglycan factor (top) and collagen factor (bottom) over percentage of width from anterior to posterior with SEM in color.

Figure 5. Left: distribution of the proteoglycan factor for four intervertebral discs of experiment 2. Right: Safranin O staining of nearby slices of the same four intervertebral discs. With this staining, proteoglycans are shown in red.

Figure 6. Average proteoglycan and collagen factor over percentage of width from anterior to posterior, with SEM in color.

585 **Table 1.** Average proteoglycan and collagen content Experiment 1

	Whole disc control	Whole disc degenerated	Difference [95% CI]	Nucleus control	Nucleus degenerated	Difference nucleus [95% CI]	Anterior annulus control	Anterior annulus degenerated	Difference anterior annulus [95% CI]
Average Proteoglycan content	0.224	0.179	-0.045 [-0.09,- 0.00]	0.302	0.242	-0.060 [-0.119,- 0.001]	0.080	0.061	-0.019 [-0.038, 0.000]
Average Collagen content	0.054	0.086	0.031 [0.013,0.05]	0.0437	0.0751	0.0314 [-0.058,- 0.005]	0.071	0.111	-0.040 [-0.0150, - 0.0642]
Proteoglycan/ Collagen ratio	4.38	2.26	-2.12 [-3.73, -0.52]	8.17	3.71	-4.46 [-9.11,- 0.19]	1.41	0.58	-0.84 [-1.47,- 0.20]

586

Table 2. Median [minimum-maximum] for the histological degenerative gradings. Safranin O histological staining on nearby slices of the same intervertebral disc (Fig. 5) showed similar distribution as the intervertebral discs from experiment 2, confirming that this factor indeed identifies proteoglycan.

Loading group	Method by Hoogendoorn et al. ¹¹	Method by Sive et al. ¹⁹
Control loading	2.3 [0.0-3.0]	2.0 [1.0-3.5]
Overloading	2.3 [0.5-3.5]	1.3 [0.5-3.0]
T=0	1.8 [0.0-2.5]	1.8 [1.0-3.0]

593 **Table 3.** Collagen entropy of different sections of the discs of experiment 1, divided into 10
594 equal parts from anterior to posterior.

Percentile anterior- posterior width	Entropy healthy (SD)	Entropy degenerated (SD)	P-value
0-10	4.3 (0.8)	5.1 (0.3)	0.06
10-20	4.4 (0.7)	5.3 (0.3)	0.03
20-30	3.3 (0.6)	4.6 (0.4)	<0.01
30-40	3.0 (0.8)	4.0 (0.5)	0.01
40-50	3.0 (0.8)	4.1 (0.5)	0.04
50-60	2.9 (1.1)	4.1 (0.7)	0.07
60-70	3.2 (1.3)	4.0 (0.4)	0.13
70-80	3.4 (0.7)	3.8 (0.5)	0.05
80-90	3.7 (0.8)	3.7 (0.3)	0.81
90-100	1.7 (1.9)	1.6 (2.0)	0.92

595
596

Figure 1

[Click here to download high resolution image](#)

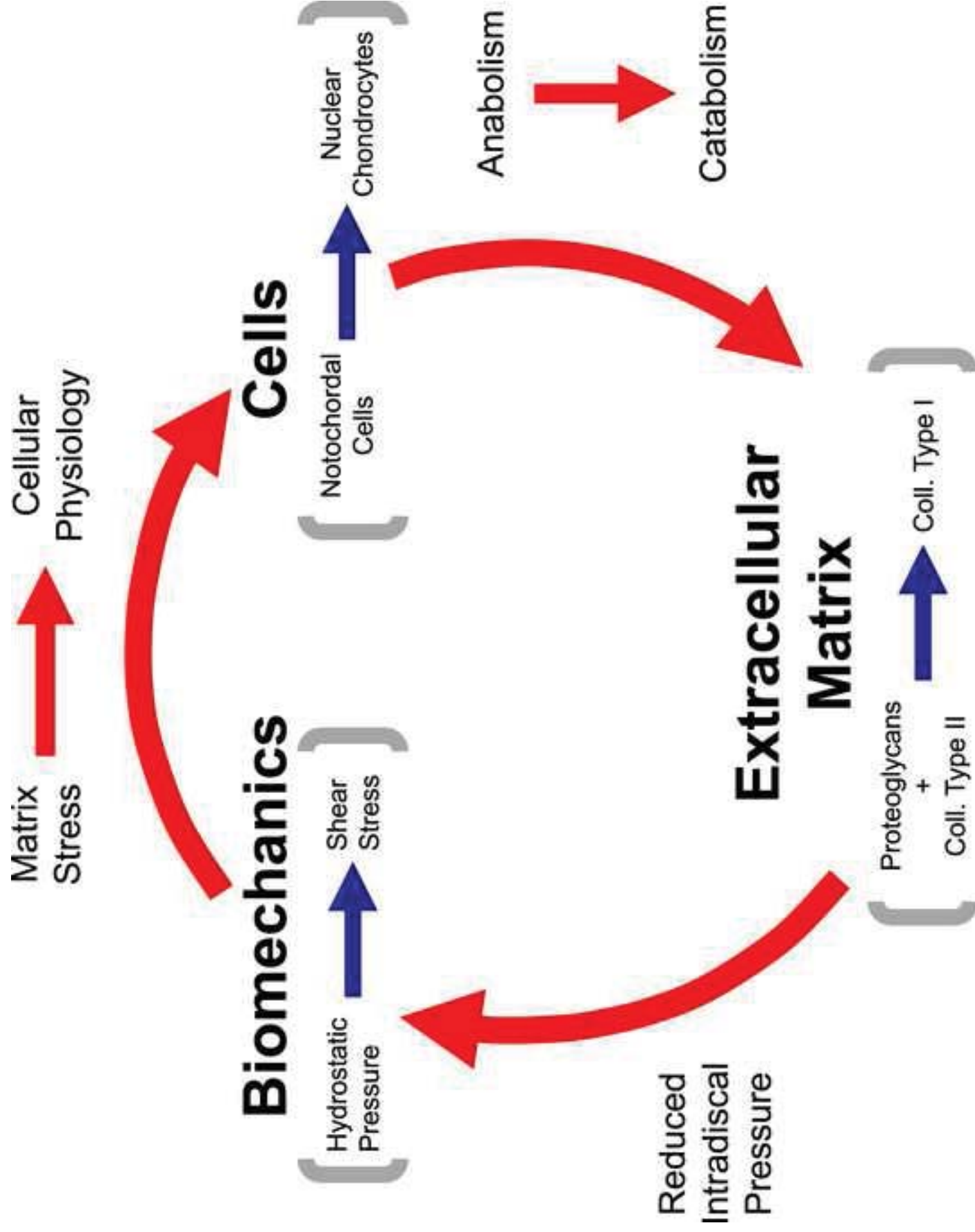


Figure 2a
[Click here to download high resolution image](#)

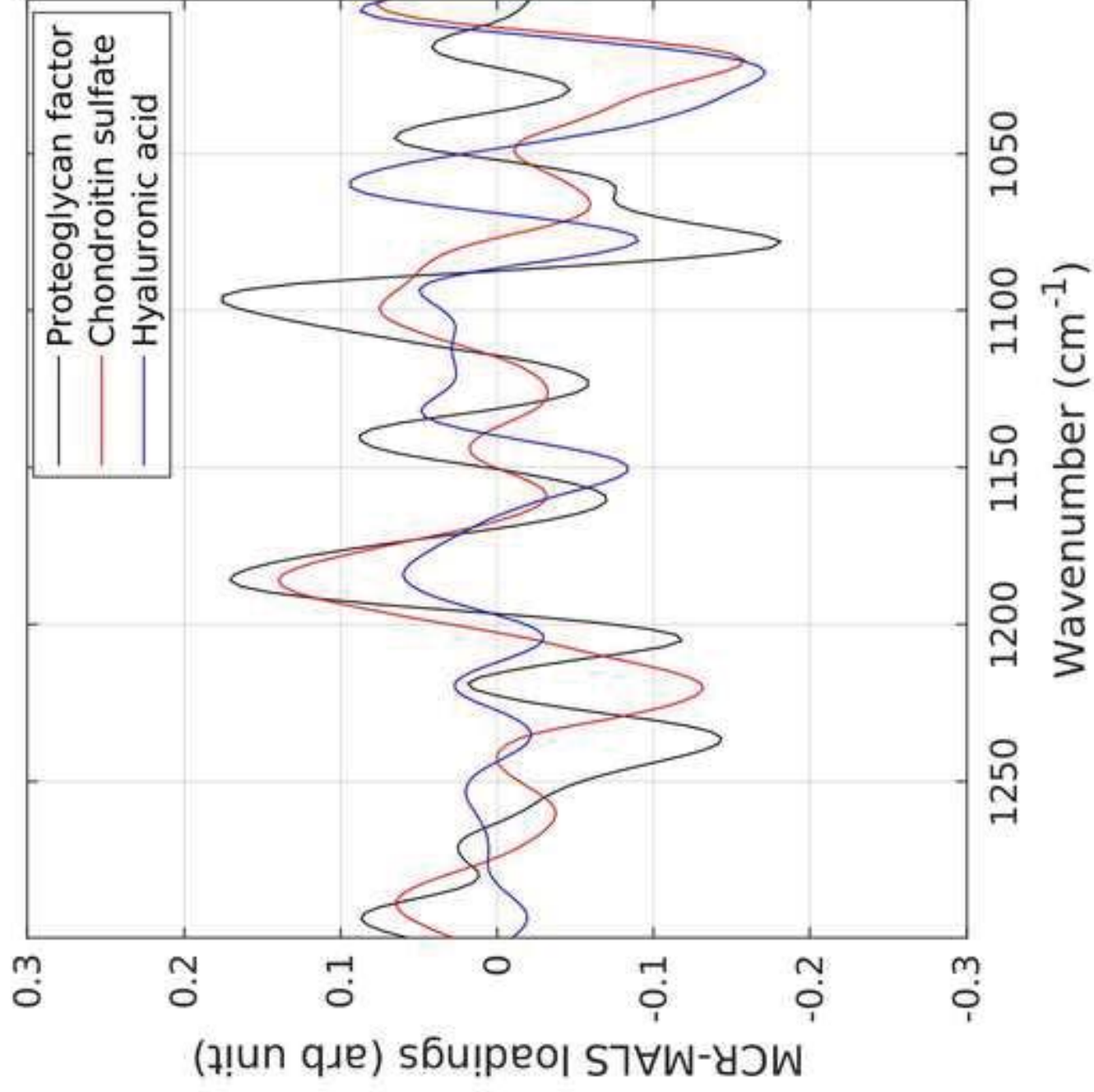


Figure 2b
[Click here to download high resolution image](#)

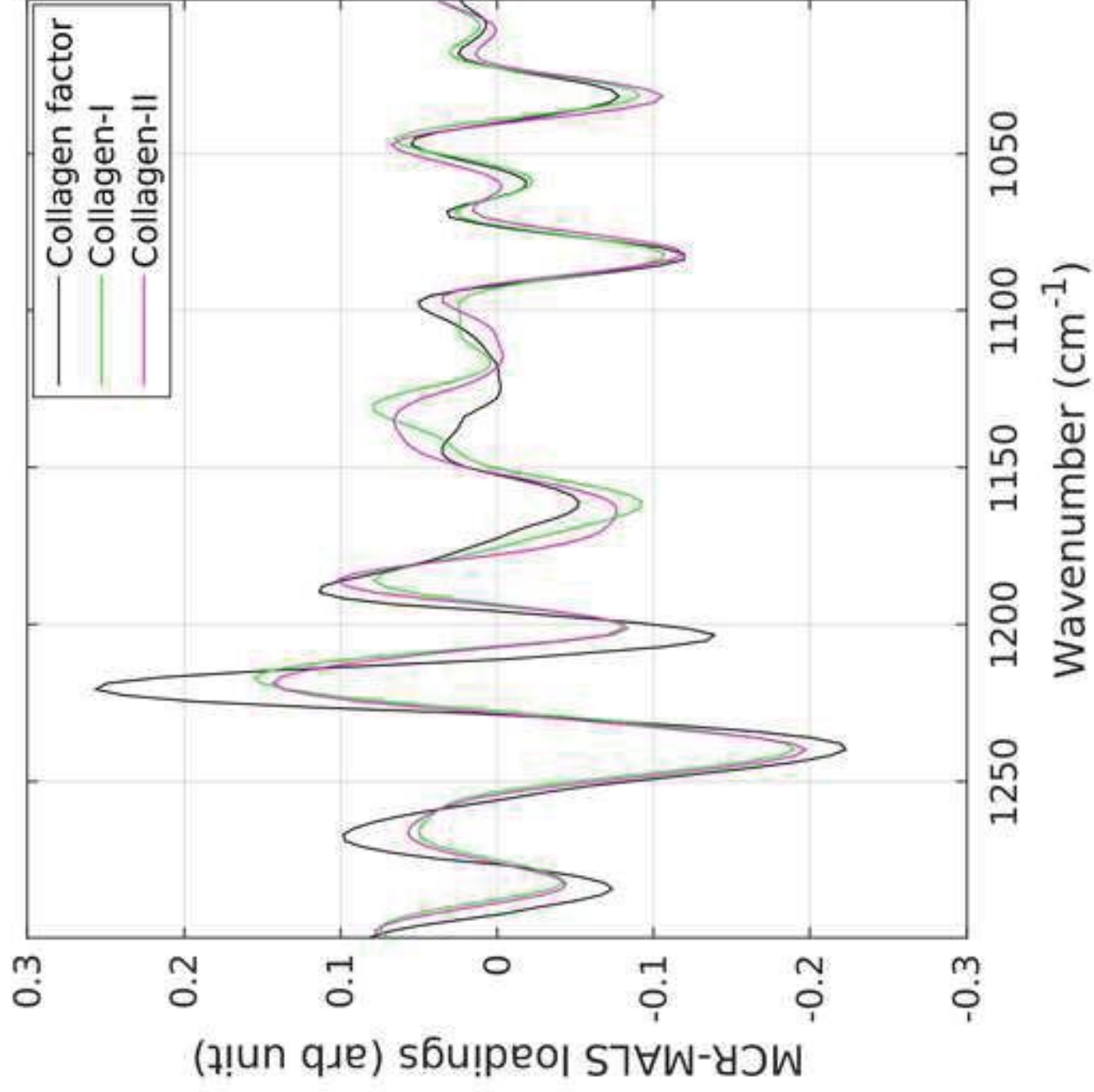


Figure 3
[Click here to download high resolution image](#)



Figure 4
[Click here to download high resolution image](#)

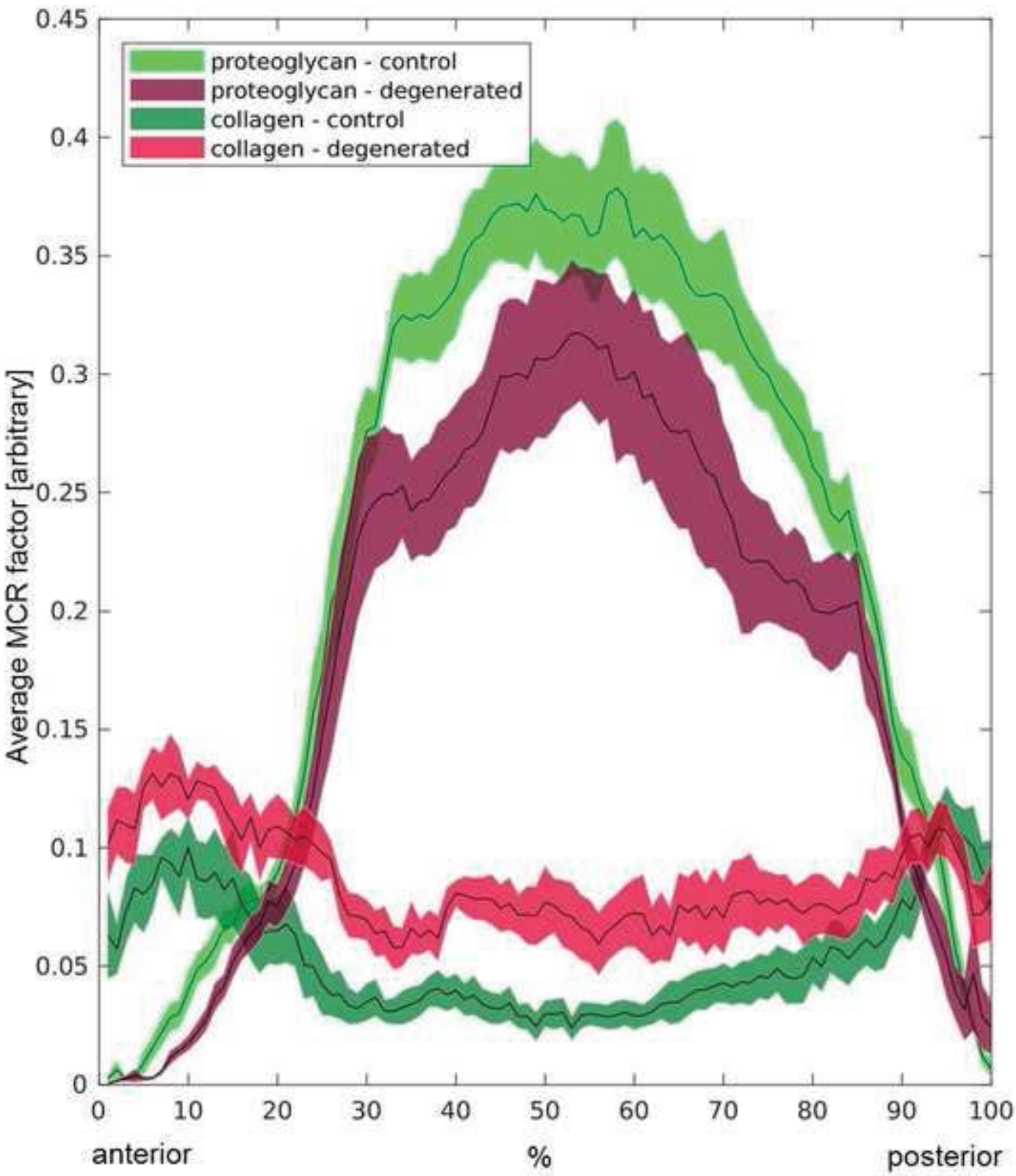


Figure 5
[Click here to download high resolution image](#)

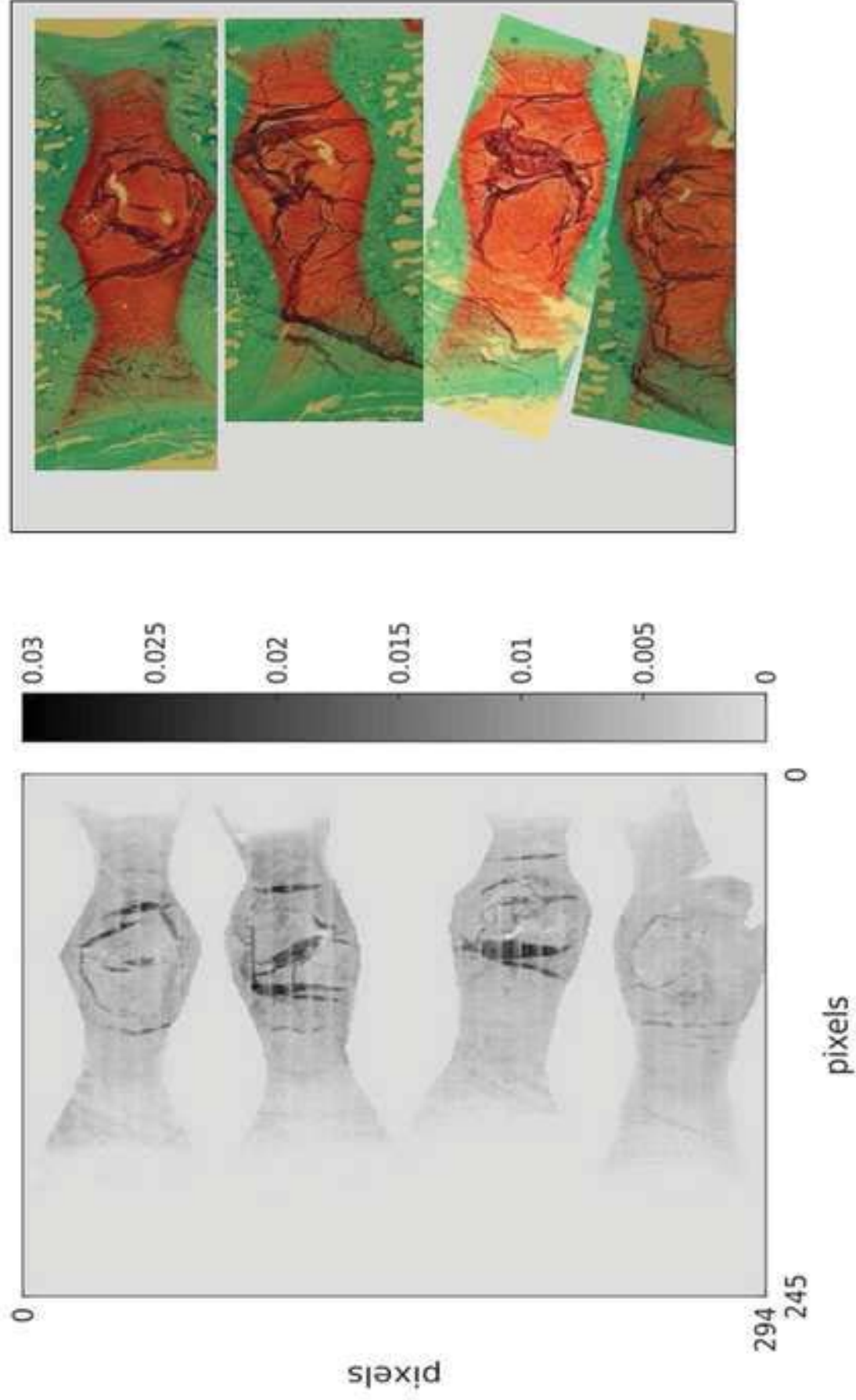


Figure 6
[Click here to download high resolution image](#)

